

First estimate of the time delay in HE 1104–1805^{*}

Lutz Wisotzki¹, Olaf Wucknitz¹, Sebastian Lopez¹, and Anton Norup Sørensen²

¹ Hamburger Sternwarte, Universität Hamburg, Gojenbergsweg 112, 21029 Hamburg, Germany

² Copenhagen University Observatory, Juliane Maries Vej 30 DK-2100 Copenhagen, Denmark

Received; accepted

Abstract. We present first results from five years of spectrophotometric monitoring of the bright double QSO and gravitational lens HE 1104–1805. The quasar has varied considerably over this time, while the emission line fluxes appear to have remained constant. We have constructed monochromatic continuum light curves for components A and B, finding that B leads the variability. A quantitative analysis with the Pelt method gives a best estimate for the light travel time delay of about 0.73 years, although a value as low as 0.3 cannot yet be excluded. We discuss possible models for the QSO-lens configuration and use our measured time delay to predict the redshift of the lens, z_d . Finding that most likely $z_d \lesssim 1$, we can rule out the hitherto favoured values of $z_d = 1.32$ or 1.66 . A new candidate is an absorption system at $z = 0.73$, but the lens could also be an elliptical not detected in absorption.

Key words: Quasars: individual: HE 1104–1805 – Quasars: general – Gravitational lensing

1. Introduction

HE 1104–1805 (the ‘Double Hamburger’, $z = 2.32$) is one of the brightest multiply imaged QSOs in the sky: Around discovery in 1993, its *B* band magnitudes were 16.7 and 18.6 for components A and B, respectively (Wisotzki et al. 1993). The gravitational lens nature is now firmly established, after the deflecting galaxy has been detected in the line of sight (Courbin et al. 1998; Remy et al. 1998, quoted as R98 in the following), but the lens redshift is still unknown. The strong $z = 1.66$ damped Ly α system in component A (Smette et al. 1995) may be an obvious candidate, but the observed properties do not agree well with this hypothesis (R98; Lopez et al. 1998).

Because of their brightness and the relatively large image separation of $3''2$, photometry of the two components can be obtained under less than optimal circumstances, especially as HE 1104–1805 shows variability with considerable amplitude (Wisotzki et al. 1995). The system is therefore well-suited

for systematic monitoring, with the ultimate aim to obtain the light travel time delay and to estimate the Hubble parameter. We have started with a *spectrophotometric* monitoring in early 1996, and including some earlier observations the time span covered is now five years. Here we present first results from this monitoring campaign, focused specifically on the issue of time delay estimation. Other aspects of the monitoring, in particular a comparison of continuum and emission line properties and the possible signatures of microlensing, will be dealt with in a future paper.

2. Observations and data reduction

The spectrophotometric monitoring was conducted at the ESO 3.6 m telescope in service mode. Typically once a month during the visibility period, up to one hour was dedicated to the programme. The instrument was EFOSC1 with 512×512 pixels Tektronix CCD until June 1997, and EFOSC2 with a $2K \times 2K$ Loral/Lesser chip afterwards. The observations always comprised one or several acquisition images, followed by a low-resolution spectrum with the B300 grism through a $5''$ slit aligned along components A and B. Exposure time was between 15–30 min, spectral resolution was typically $\sim 20 \text{ \AA}$, and the spectra covered the wavelength range between 3800 \AA and 7000 \AA . The seeing was between $1''.1$ and $2''.0$. A few datasets have been included in this analysis that were obtained before the proper monitoring started. Some were taken with the same configuration as described above; in addition we used the NTT data shown already by Wisotzki et al. (1993) and a set of spectra obtained with the LDS spectrograph at the Nordic Optical Telescope in February 1994.

The CCD frames were reduced in a homogeneous way, largely following standard procedures. The most critical task was to perform an unbiased simultaneous extraction of the two components. We have employed a three-step deblending algorithm, consisting of the following tasks: (1) Two Gaussians, of the same FWHM and with fixed angular separation but otherwise unconstrained, were fitted simultaneously to each spectral resolution element. (2) The variation with wavelength of the resulting parameters FWHM and centroid location was fitted by low-order polynomials. (3) Another double-Gaussian fit was performed, now with only the two amplitudes as free param-

Send offprint requests to: L. Wisotzki, lwisotzki@hs.uni-hamburg.de

^{*} Based on observations collected at the European Southern Observatory, La Silla, Chile

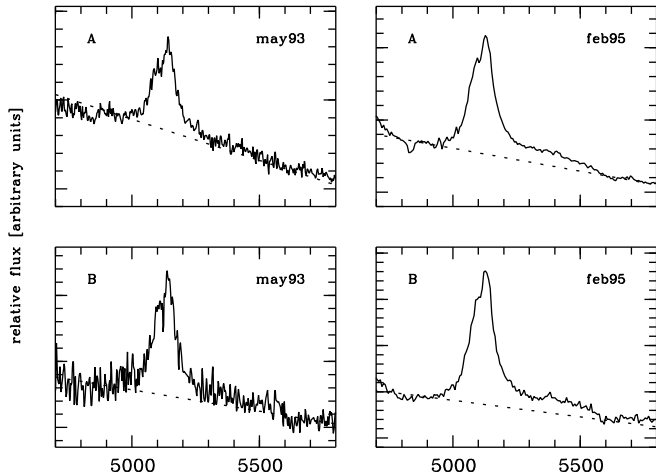


Fig. 1. Example spectra obtained in the monitoring, showing the region around C IV $\lambda 1549$ for two epochs, in components A and B. The adopted continua are marked by the dotted lines.

eters. The algorithm is described in more detail by Lopez et al. (1998). Inspection of the residual maps revealed no significant deviation from this model. The resulting one-dimensional spectra were recorded as MIDAS table files, thus avoiding loss of information due to data rebinning.

Wavelength calibration frames were obtained from comparison lamp spectra, usually based on Helium/Argon lines. The observing conditions were in many cases not photometric, and standard star spectra for flux calibration purposes were obtained in only a few nights. Therefore only a relative flux calibration could be attempted. Two of the pre-monitoring observations were made through a narrow slit, which in one case was not even aligned. We explain below how these measurements could be incorporated into the analysis.

3. Continuum light curves

Altogether, 19 sets of spectra could be secured, of which 14 were obtained in the course of the monitoring. Most spectra are of very high quality, some with a continuum S/N ratio exceeding 100 in component A. Examples of the spectra are presented in Fig. 1; the range in S/N ratio is bracketed by these example data, with most spectra looking rather similar to the February 1995 ones. The high quality of the data enabled us to monitor the *monochromatic continuum fluxes* of both components, which has the advantage over the conventional broadband magnitudes that it is a brightness measure uncontaminated by emission lines and their possibly different variability patterns. However, absolute photometric calibration from standard stars was usually not possible, and we had to design a method to compare spectra taken at different epochs. In the following we motivate and outline this procedure.

After placing the spectra on a relative flux scale, we measured the fluxes and equivalent widths of all major emission lines in both components (Ly α , Si IV $\lambda 1400$, C IV $\lambda 1549$, and C III] $\lambda 1909$). Local continua were estimated by fitting straight

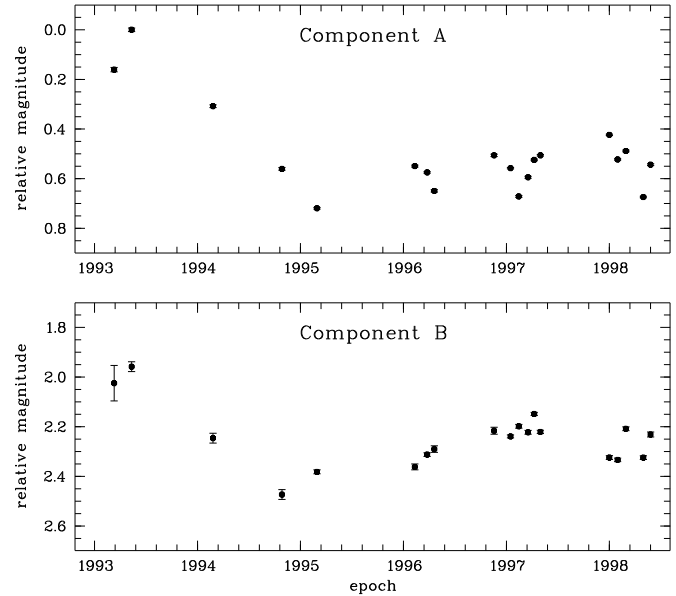


Fig. 2. Monochromatic continuum light curves of both components, taken at $\lambda_c = 4910 \text{ \AA}$. The zero point is arbitrary, but the same for both panels. Error bars in the upper panel are generally smaller than the symbol size.

lines to predefined wavebands known to be largely devoid of emission and absorption lines (cf. examples in Fig. 1). Although a direct comparison of line strengths between different epochs is not possible, there is one strong piece of evidence that the lines have remained essentially constant over the time span observed: The flux ratio between the same lines in components A and B, independent of the absolute scale, has stayed at a consistently constant value of 2.85 ± 0.07 for all lines. This implies either a time delay of much less than a month (the separation between data points during the periods of quasi-continuous monitoring), which is highly improbable, or simply constancy of the line fluxes as such. Adopting the latter hypothesis, we were then able to recalibrate the spectra by scaling them to equal emission line fluxes. As reference we used C IV, a prominent line that is surrounded by clearly identifiable continuum windows visible also at low spectral resolution.

For each pair of spectra we computed a scale factor so that the C IV flux of component A assumed an arbitrary but constant value, and applied this factor to both spectra. The average continuum values in the interval $4880 \text{ \AA} < \lambda < 4940 \text{ \AA}$, thus at $\lambda_c = 4910 \text{ \AA}$, were then determined for A and B. This estimate of the QSOs brightness is independent of external flux standards and of photometric conditions, and we were thus able to incorporate also narrow slit observations by the same method. Note that the relative flux calibration based on standard stars was not even strictly needed, although it helped in removing the instrumentally caused curvature from the spectra. The resulting light curves are depicted in Fig. 2. The error bars in this plot contain both the continuum uncertainties due to photon shot noise and the error of the line flux rescaling factor. The zeropoint for both components is arbitrarily set at the continuum

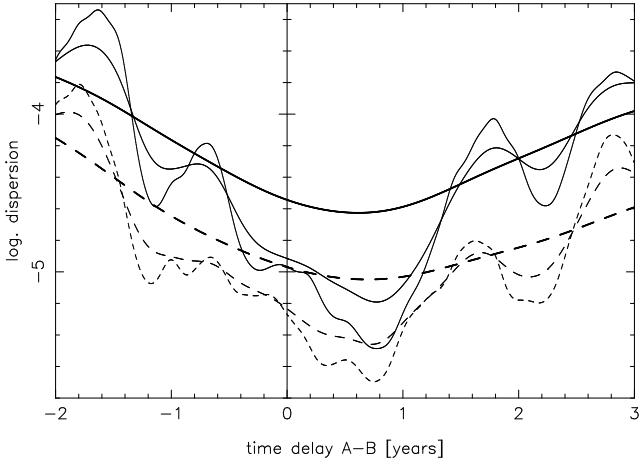


Fig. 3. Dispersion curves for decorrelation lengths of 50 (thin), 100 (normal), and 365 (thick lines) days. For the solid lines, the dispersion was calculated using statistical weights from the measurement errors. For the dashed lines, constant weights were used.

magnitude of A in May 1993, which constitutes the brightest point.

Although the light curve is certainly not well-sampled, some features are very clearly discernible. The strong decline in component A between 1993 and 1995, spanning almost a magnitude, is well mirrored in B, except for the inflection between Nov 1994 and Feb 1995 which occurs only in B. This feature alone is already very suggestive that B leads the variability, as one expects from the observed lens configuration (cf. R98). From early 1996 on, the sampling improved due to the beginning of regular monitoring, and it became apparent that the object shows also significant variability on relatively short time scales.

4. Time delay estimation

Sliding the light curves against each other to find the best visual agreement lead us to an estimate of about half a year for the time delay A–B (component B leading) with a brightness difference of about 1.7 mag. For such a time delay, the observing periods of the one component coincide more or less with the seasonal gaps in the light curve of the other. This effect without doubt produces a bias for values around $\Delta t \approx 0.5$ yr, and we had to find a quantitative method of estimation that is insensitive to such biases.

The dispersion method of Pelt et al. (1994; 1996) proved to be quite robust despite the windowing effects in the case of time delay determination for the double quasar 0957+561. To minimise the bias for our data, we used the dispersion $D_{4,3}$ (Pelt et al. 1996) which takes into account not just neighbouring data but uses the complete light curves with weight factors corresponding to the (shifted) time differences of two observations each. If the decorrelation length β is chosen sufficiently large, the windowing effect becomes increasingly less signif-

Table 1. Relative positions of the images and the lensing galaxy, taken from the CASTLES compilation (Kochanek et al. 1998; Lehár et al., in preparation). The directions of positive x and y are west and north, respectively.

	x ["]	y ["]
A	0.0	0.0
B	-2.901 ± 0.003	-1.332 ± 0.003
G	-0.974 ± 0.003	-0.510 ± 0.003

Table 2. Parameters for the SIST and the SIEMD model: α_0 is the Einstein radius, ϵ and γ are ellipticity and shear, with position angles θ and ϕ , respectively. M_A and M_B are the magnifications, the signs giving the parity, and T contains the time delay according to Eq. 1.

model	α_0 ["]	ϵ θ [°]	γ ϕ [°]	M_A M_B	T [arcsec ²]
SIST	1.403	0.	0.122 112.1	-7.23 +2.52	1.395
SIEMD	1.546	0.191 22.1	0.	-7.12 +2.48	1.590

icant. Figure 3 shows the dispersion for different values of β over an interval of *a priori* possible time delays.

The global minima of all dispersion curves are consistently located between 0.6 and 0.8 years, which indicates a value of the time delay in this range. Using a decorrelation length of 100 days which reduces the windowing but does not smooth the data on longer time scales, the minimum is at $\Delta t = 0.73$ yr with magnitude difference of 1.70 for the weighted data. Note that the existence of slightly weaker local minima still permit a somewhat smaller time delay of 0.3–0.5 yrs. On the other hand, a Δt of one year or more is not consistent with the data.

This estimate of a time delay is to be seen as a very preliminary result. A detailed analysis of the light curves has to wait until better sampled data are available.

5. Modeling the deflector potential

The observational parameters of this system are the image and galaxy positions (cf. table 1), and the flux ratio of the images. For the latter it is important to realise that the continuum ratio of 4.8 (1.7 mag) differs from the emission line value because of the excess continuum component in image A, tentatively identified with microlensing by Wisotzki et al. (1993). We use the flux ratio of 2.85 obtained from the emission lines (see above), which should be much less affected by microlensing than the continuum because of the larger size of the emitting region.

As a reference model, we use a singular isothermal sphere with external shear (SIST). This is probably the simplest model capable to reproduce the observed positions and the flux ratio (cf. R98). The parameters of this model can be found in Table 2. The observational uncertainties lead to an internal error of only

0.6 % for the time delay. To examine the much larger possible errors due to the modeling, we used a more general approach of models consisting of a singular isothermal ellipsoidal mass distribution (SIEMD, see Kassiola & Kovner 1993) with external shear. For the model-fitting we fixed ellipticity ϵ and shear γ , and used the other parameters listed in Table 2 (including the position angles) and the source position to fit the observations. Due to the small number of constraints, the position of the lensing galaxy was fixed at the observed values. This was carried out for a range of values for ϵ and γ . With the restriction of $\epsilon < 0.3$ and $\gamma < 0.2$, we find a maximum deviation of +20 % and -10 % for the time delay. As an example, the model with zero external shear is also given in Table 2. The time delay for this case is 14 % larger than for the SIST model.

6. Implications for the lensing galaxy

If the redshift of the lens z_d were known, we could compute the Hubble parameter from the time delay using the fundamental equation connecting the time delay Δt and the parameter T

$$\Delta t = H_0^{-1} (1 + z_d) \frac{d_d d_s}{d_{ds}} T \quad . \quad (1)$$

As z_d is still unknown, we cannot use this formula to get H_0 . However, simply *adopting* a canonical value for H_0 allows us to predict the redshift of the lens, or better, to constrain the range of possible values for z_d . Figure 4 shows the product of time delay and Hubble parameter as a function of z_d . For $\Delta t = 0.73$ yr, $H_0 = 50 \text{ km s}^{-1} \text{ Mpc}^{-1}$, $\Omega = 1$, and $\lambda = 0$, the SIST model predicts $z_d = 0.79$, and the velocity dispersion of the galaxy for this model is $\sigma_v = 332 \text{ km s}^{-1}$. This corresponds to a mass of $9.2 \cdot 10^{11} M_\odot$ inside of one Einstein radius, well within the range expected for a reasonably massive galaxy. With an I_c band magnitude of 20.9 according to R98, the mass-to-light ratio would then be of the order of 10 solar units, again quite consistent with the expectations for such a galaxy (cf. Keeton et al. 1998).

Recently, values for the time delay have been predicted based on the assumption that one of the two strong metal absorption line systems at $z = 1.32$ or $z = 1.66$ can be identified with the deflector. R98 give $\Delta t \simeq 1.9 h_{50}^{-1}$ yrs, Courbin et al. (1998) even $3.5 h_{50}^{-1}$ yrs. Since we can reliably exclude $\Delta t > 1$ yr, our results are not compatible with z_d significantly larger than 1; in particular, the absorbers at 1.32 and 1.66 can be ruled out.

We have searched our higher resolution NTT spectra of HE 1104–1805 (cf. Lopez et al. 1998) for absorption lines within the redshift range permitted by Fig. 4. An additional demand is that the lines should be stronger in A, as this component is located closer to the deflector. Two Mg II absorption systems, at $z = 0.52$ and 0.73 , meet the criteria. Of these, $z_d = 0.52$ is acceptable only for a time delay as short as ~ 0.4 yrs, and is furthermore not compatible with the $I - K$ colour estimate of R98. This leaves the system at $z = 0.73$ as candidate; however, the lens could also be an elliptical galaxy for which Mg II ab-

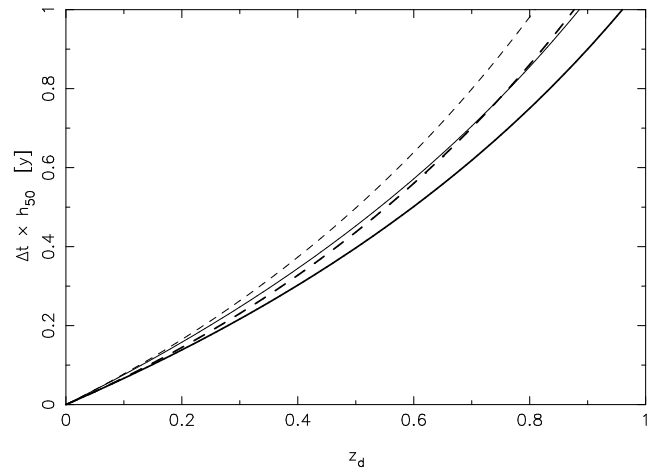


Fig. 4. Time delay scaled by H_0 for the SIST (thick) and SIEMD (thin) model. Standard Einstein-de Sitter cosmology is shown as solid lines, a low-density universe ($\Omega = 0.3, \lambda = 0$) as dashed lines. Flat low-density world models are located between these two curves.

sorption would be a poor indicator. The very red colours measured by R98 support such a notion.

Acknowledgements. We are grateful to all ESO staff and visiting astronomers for their cooperation in obtaining the monitoring data. We also thank Dr. P. Schechter for enlightening discussions and Dr. E. Falco for providing us with the latest astrometric data of the system.

References

- Courbin F., Lidman C., Magain P., 1998, *A&A* 330, 57
- Kassiola A., Kovner I., 1993, *ApJ* 417, 450
- Keeton C.R., Kochanek C.S., Falco E.E., 1998, *ApJ* in press, astro-ph/9708161
- Kochanek C.S., Falco E.E., Impey C., et al., 1998, CASTLe Survey, <<http://cfa-www.harvard.edu/castles/>>
- Lopez S., Reimers D., Rauch M., Sargent W.L.W., Smette A., 1998, *ApJ* in press, astro-ph/9806143
- Pelt J., Hoff W., Kayser R., Refsdal S., et al., 1994, *A&A* 286, 775
- Pelt J., Kayser R., Refsdal S., Schramm T., 1996, *A&A* 305, 97
- Remy M., Claeskens J.-F., Surdej J., Hjorth J., et al., 1998, *New Astronomy* 3, 379
- Smette A., 1995, in: *QSO Absorption Lines*, ed. G. Meylan, ESO Astrophysics Symposia, 275
- Wisotzki L., Köhler T., Kayser R., Reimers D., 1993, *A&A* 278, L15
- Wisotzki L., Köhler T., Ikononou M., Reimers D., 1995, *A&A* 297, L59